Title

Expression and role of Elovl4 elongases in biosynthesis of very long-chain fatty acids during zebrafish *Danio rerio* early embryonic development

Authors

Óscar Monroig[a]; Josep Rotllant[b]; José M. Cerdá-Reverter[c]; James R. Dick[a]; Antonio Figueras[b]; Douglas R. Tocher[a]

Addresses

[a] Institute of Aquaculture, University of Stirling, Stirling FK9 4LA, Scotland, UK

[b] Instituto de Investigaciones Marinas. CSIC. 36208 Vigo, Pontevedra, Spain

[c] Instituto de Acuicultura Torre de la Sal. CSIC. 12595 Cabanes, Castellón, Spain

Corresponding author

Óscar Monroig

Institute of Aquaculture, University of Stirling, Stirling FK9 4LA, Scotland, U.K.

Tel: +441786 467993; Fax: +44 1786 472133; E-mail: oscar.monroig@stir.ac.uk

Keywords

Development; elongation; Elovl4; fatty acid metabolism; very long-chain fatty acids; very long-chain polyunsaturated fatty acids; zebrafish.

Summary

Elovl4 is a fatty acyl elongase that participates in the biosynthesis of very long-chain fatty acids (≥C24), which are relatively abundant in skin (saturated chains), or retina, brain and testes (polyunsaturated chains) of mammals. In the present study we characterised two Elovl4 proteins, Elovl4a and Elovl4b, from zebrafish *Danio rerio*, and investigated their expression patterns during embryonic development. Heterologous expression in baker's yeast showed that both zebrafish Elovl4 proteins efficiently elongated saturated fatty acids up to C36, with 26:0 appearing the preferred substrate as reported for human ELOVL4. Interestingly, activity for the elongation of PUFA substrates was only shown by Elovl4b, which effectively converted eicosapentaenoic (20:5n-3) and arachidonic (20:4n-6) acids to elongated polyenoic products up to C36. Furthermore, zebrafish Elovl4b may be involved in the biosynthesis of docosahexaenoic acid (22:6n-3, DHA) as it had the capacity to elongate 22:5n-3 to 24:5n-3 which can be subsequently desaturated and chain shortened to DHA in peroxisomes. The distinct functional roles of zebrafish Elovl4 proteins were also reflected in their spatial-temporal expression patterns during ontogeny. Analyses by whole-mount *in situ* hybridisation in zebrafish embryos showed that *elovl4a* was expressed in neuronal tissues (wide-spread distribution in the head area), with *elovl4b* specifically expressed in epiphysis (pineal gland) and photoreceptor cells in the retina. Similarly, tissue distribution in adults revealed that *elovl4a* transcripts were found in most tissues analysed, whereas *elovl4b* expression was essentially restricted to eye and gonads. Overall, the results suggest that zebrafish *elovl4b* resembles other mammalian orthologues in terms of function and expression patterns, whereas *elovl4a* may represent an alternative elongase not previously described in vertebrates.

Introduction

Elongases of very long-chain fatty acids (Elovl) are the initial and rate-limiting enzymes responsible for the condensation reaction required for biosynthesis of long-chain fatty acids (FA) [1]. Seven members of the Elovl family, termed ELOVL 1-7, have been identified in mammals that differ from each other in their substrate specificity [2-4]. Generally speaking, mammalian ELOVL1, ELOVL3, ELOVL6 and ELOVL7 are involved in elongation of saturated and monounsaturated FAs, whereas ELOVL2 and ELOVL5 elongate polyunsaturated fatty acids (PUFAs). The functional role of ELOVL4 in fatty acid biosynthesis was later ascertained.

ELOVL4 was first identified as a gene causing a dominant form of Stargardt-like macular dystrophy (STGD3). Three distinct mutations in the last exon (exon-VI), a 5-bp [5], two 1-bp [6], and a nonsense mutation [7] in the *ELOVL4* gene were predicted to introduce a premature stop codon resulting in a truncated ELOVL4 protein lacking the putative endoplasmatic reticulum (ER) dilysine retention signal (KXKXX). Subsequent investigations revealed that truncated ELOVL4 is not retained in the ER and misplaces wild type ELOVL4 to non-ER aggregates [8-10]. In addition to its localisation in the ER, the site of long-chain fatty acid synthesis [11], the similarities between the amino acid sequence of human ELOVL4 with other elongase family proteins and its high expression levels in tissues having high requirements for very long-chain fatty acids (VLC-FA), suggested a role for ELOVL4 in FA biosynthesis.

Previous investigations demonstrated that ELOVL4 is required for generating saturated VLC-FAs (i.e. carbon chain $C \geq 28$) that are components of sphingolipids and ceramides [12-15]. Additionally, ELOVL4 was speculated to participate in the synthesis of very long-chain PUFAs (VLC-PUFAs), as STGD3 mutation reduced

retinal levels of C32-C36 acyl phosphatidylcholines (PCs) in mouse retinal extracts [16]. The dual role of human ELOVL4 was recently confirmed by Agbaga and co-workers who demonstrated that the enzyme is active both in the elongation of saturated VLC-FA 26:0 to 28:0 and 30:0, and in the biosynthesis of VLC-PUFAs ranging from C28-C38 [17].

Saturated VLC-FAs are abundant compounds in the epidermis of mammals, where they perform essential structural functions in the maintenance of skin permeability [18]. Although less clear, the functions of VLC-PUFAs appear to be related to their unusually long aliphatic chains (C24-C38) and the concomitant characteristic that some VLC-PUFAs possess by combining the properties of saturated fatty acid in the proximal end with those of PUFA in the distal end [17]. Thus, VLC-PUFAs are compounds uniquely found in specific lipid molecules of retina [19,20], brain [21,22] and testis [23-25].

Since their discovery more than two decades ago, studies of VLC-FA and their metabolism in vertebrates have revealed their prominent role in processes such as vision, brain functioning, reproduction and skin permeability [19,22,26]. It is thus important to investigate the molecular mechanisms underlying the biosynthetic pathways of VLC-FA in early developmental stages at the onset of many of these physiological processes. Zebrafish (*Danio rerio*), a popular model organism in vertebrate developmental biology, has recently been used to study several aspects of lipid metabolism [27-30]. Zebrafish possess two genes encoding putative Elovl4 elongases, termed as *elovl4a* (gb|NM_200796|) located in chromosome 16 and *elovl4b* (gb|NM_199972|) in chromosome 23. Their functional roles and expression profiles during ontogeny were unknown.

The present study aimed to characterise the two putative Elovl4 enzymes from *Danio rerio*, and to investigate their expression patterns during development. Firstly, we isolated both *elovl4* cDNAs, *elovl4a* and *elovl4b*, analysed their sequences, and studied their function by expressing their open reading frames (ORF) in recombinant yeast incubated with appropriate fatty acid substrates. Subsequently, the spatial-temporal expression patterns of *elovl4a* and *elovl4b* were investigated during zebrafish embryogenesis, in order to identify the distinct biological processes the genes are involved in during early development of vertebrates.

Materials and methods

Fish maintenance

Zebrafish embryos were cultured as previously described [31] and staged by standard criteria [32] or by hours (hpf) or days (dpf) post fertilisation. Experiments were performed using the AB wild-type strain. For whole-mount *in situ* hybridisation analyses, dechorionated embryos were fixed overnight at 4 ºC in 4 % paraformaldehyde in 1xPBS, washed in PBS, and dehydrated through a methanol series, and stored at -20 ºC in 100 % methanol. To inhibit embryo pigmentation, embryo medium was supplemented with 0.003 % 1-phenyl-2-thiourea (PTU, Sigma) [31].

Zebrafish elovl4: cloning and functional characterisation by heterologous expression in Saccharomyces cerevisiae

PCR fragments corresponding to the ORF of the putative zebrafish *elovl4a* (gb|NM_200796|) and *elovl4b* (gb|NM_199972|) were amplified from ovary and whole-eye cDNA, respectively, using the high fidelity Pfu Turbo DNA polymerase

(Stratagene, Agilent Technologies, Cheshire, UK). A nested PCR approach was used with a first round performed with specific primer pairs (Table 1) Elovl4aU5F / Elovl4aU3E (*elovl4a*) and Elovl4bU5F / Elovl4bU3E (*elovl4b*). PCR conditions consisted of an initial denaturing step at 95 ºC for 2 min, followed by 33 cycles of denaturation at 95ºC for 30 s, annealing at 58 (*elovl4a*) or 55 ºC (*elovl4b*) for 30 s, extension at 72 ºC for 1 min 20 s, followed by a final extension at 72 ºC for 5 min. First round PCR products were used as template for the nested PCR with thermal conditions as described above, and with primers containing restriction sites (underlined in Table 1) Elovl4bVF (*Hin*d III) and Elovl4aVR (*Xho* I) for *elovl4a* and Elovl4bVF (*Hin*d III) and Elovl4bVR (*Xho* I) for *elovl4b*.

The DNA fragments containing zebrafish *elovl4* forms were then digested with the corresponding restriction endonucleases (New England BioLabs, Herts, UK) and ligated into a similarly restricted pYES2 yeast expression vector (Invitrogen, Paisley, UK). The purified plasmids (GenElute™ Plasmid Miniprep Kit, Sigma) containing the putative *elovl4* ORFs were used to transform *S. cerevisiae* competent cells (S.c. EasyComp Transformation Kit, Invitrogen). Transformation and selection of yeast with recombinant pYES2-*elovl4* plasmids and yeast culture were performed as described in detail previously [33,34]. Briefly, cultures of recombinant yeast were grown in *S. cerevisiae* minimal medium-uracil supplemented with one of the following FA substrates: lignoceric acid (24:0), eicosapentaenoic acid (20:5n-3), arachidonic acid (20:4n-6), docosapentaenoic acid (22:5n-3), docosatetraenoic acid (22:4n-6) or docosahexaenoic acid (22:6n-3). Docosapentaenoic and docosatetraenoic acids (>98-99 % pure) were purchased from Cayman Chemical Co. (Ann Arbor, USA) and the remaining FA substrates (>99 % pure) and chemicals used to prepare the *S. cerevisiae* minimal medium-uracil were from Sigma Chemical Co. Ltd. (Dorset,

UK). Lignoceric acid was dissolved in α-cyclodextrin [35] at 5 μM and added to the yeast cultures at a final concentration of 0.6 μM, whereas PUFA substrates were added at final concentrations of 0.75 (C20) and 1.0 (C22) mM. After 2 days, yeast were harvested and washed for further analyses. Yeast transformed with pYES2 containing no insert were cultured under the same conditions as a control treatment.

FAME analysis by GC-MS

Total lipids from yeast were extracted by homogenisation in chloroform/methanol (2:1, v/v) containing 0.01% BHT as antioxidant. FA methyl esters (FAMEs) were subsequently prepared, extracted and purified [33]. FAMEs were identified and quantified using a gas chromatograph (GC8000) coupled to an MD800 mass spectrometer (ThermoFisher Scientific, Hemel Hempstead, UK). Samples were applied by on-column injection using an AS800 autosampler (ThermoFisher Scientific, Hemel Hempstead, UK). The gas chromatograph was equipped with a ZB-Wax silica capillary column (30 m x 0.32 mm x 0.25 μm; Phenomenex, Macclesfield, UK). Helium carrier gas was used with a column head pressure of 15 psi. The oven temperature was programmed to rise from 80 to 260 $^{\circ}$C. The GC-MS was operated in the electron ionisation (EI) single ion monitoring (SIM) mode. The 24:0, 26:0, 28:0, 30:0, 32:0, 34:0 and 36:0 response values were obtained by using the *m/z* ratios 382.4 410.4, 438.4, 466.5, 494.5, 522.5 and 550.5, respectively. For VLC-PUFA analysis, the response values were obtained by using the *m/z* ratios 79.1, 108.1 and 150.1 in SIM mode. Elongation rates from PUFA substrates were calculated by the proportion of substrate FA converted to elongated FA product as [product area/(product area + substrate area)] x 100. Conversion rates from 24:0 were not calculated as yeast endogenously contains several of the FA involved in the elongation pathway.

Alternatively, individual ≥ C24 saturated FA contents from *elovl4*-transformed yeast were calculated and compared to control yeast.

Sequence and phylogenetic analysis of Elovl4

The amino acid (AA) sequences deduced from *Danio rerio* Elovl4a (gb|NP_957090.1|) and Elovl4b (gb|NP_956266.1|) cDNAs were aligned using ClustalW2, and compared with other orthologues of human (gb|NP_073563.1|), mouse (gb|NP_683743.2|) and rat (gb|XP_001062735.1|) Elovl4s, bird *Taenopygia guttata* (gb|XP_002188735.1|) and *Gallus gallus* (gb|XP_419868.2|), and fish *Tetraodon nigroviridis* (emb|CAG01780|) and *Takifugu rubripes* (derived from EST emb|ENSTRUT00000011027|) predicted Elovl4-like proteins using the EMBOSS Pairwise Alignment Algorithms tool (http://www.ebi.ac.uk/Tools/emboss/align/). A phylogenetic tree was constructed on the basis of the AA sequence alignments between the putative zebrafish Elovl4s, vertebrate Elovl4 orthologues, and Elovl2- and Elovl5-like proteins using the Neighbour Joining method [36]. Confidence in the resulting phylogenetic tree branch topology was measured by bootstrapping through 1000 iterations.

Temporal expression of zebrafish elovl4 genes

The expression of zebrafish *elovl4* genes during the embryonic development was studied by reverse transcriptase PCR (RT-PCR). Total RNA was extracted from pools of 20-30 embryos collected at 0, 2, 3, 6, 9, 12, 14 and 19 hpf, and 1, 2, 3, 4, 5, 6 and 7 dpf using Tri Reagent (Sigma) according to manufacturer's protocol. Five µg of total RNA was reverse transcribed into cDNA using M-MLV reverse transcriptase first strand cDNA synthesis kit (Promega, Madison, USA). RT-PCRs performed on cDNA

samples consisted of an initial denaturing step at 95 ºC for 2 min, followed by 35 cycles of denaturation at 95 ºC for 30 s, annealing at 60 ºC for 30 s, and extension at 72 ºC for 1 min, followed by a final extension at 72 ºC for 5 min. Expression of *β-actin* was also determined as reference gene [37]. Primers used for RT-PCR on embryos cDNA samples are shown in Table 1.

Spatial expression of elovl4s, whole-mount in situ hybridization

To examine the spatial expression of zebrafish Elovl4a and Elovl4b, whole-mount *in situ* hybridisation (WISH) was performed on 24, 48 and 72 hpf zebrafish embryos using Digoxygenin (DIG)-labelled antisense riboprobes as previously described [38]. Antisense riboprobes were made from linerarised partial length *D. rerio elovl4a* and *elovl4b* sequences. To increase hybridisation specificity, sequences containing part of the untranslated region (UTR) were chosen. Thus, *elovl4a* probe was 567 bp (from nt 886 to 1453) in length, containing 228 bp of coding region and 339 bp of 3'UTR (gb| NM_200796|). The *elovl4b* probe was 507 bp (from nt 144 to 650) in length, containing 469 bp of coding region and 38 bp of 5'UTR (gb|NM_199972|).

Tissue distribution of zebrafish Elovl4

Total RNA from muscle, intestine, liver, brain, gill, testis, ovary, eye, posterior kidney, heart, spleen, skin, adipose tissue, anterior kidney and whole fish was extracted and cDNA synthesised as described for embryo samples. Tissue expression of zebrafish *elovl4* elongases was analysed by RT-PCR (GoTaq Polymerase, Promega) on cDNA samples, with thermal conditions identical to those detailed above for embryos. Expression of the housekeeping *β-actin* was also determined to

check the cDNA integrity. Primers used for RT-PCR on tissue cDNA samples are shown in Table 1.

Results

Elovl4 sequence and phylogenetics

The *D. rerio* elongases *elovl4a* and *elovl4b* ORFs encode proteins of 309 and 303 AA, respectively. Zebrafish Elovl4 both possess the diagnostic histidine box HXXHH motif conserved in all elongases, five membrane spanning domains, and the endoplasmic reticulum (ER) retrieval signal RXKXX (Elovl4a) and KXKXX (Elovl4b) at the carboxyl terminus (Fig. 1). Zebrafish Elovl4a and Elovl4b proteins share, respectively, 64.4 - 65.2 % AA identity to mammalian homologues, and 62.9 - 64.8 % identity with predicted Elovl4 sequences from birds. When AA sequences of zebrafish Elovl4s are compared to fish predicted Elovl4s, two groups appear to exist, with Elovl4a and *Takifugu rubripes* Elovl4 in one group (81.1 % identity), and Elovl4b and *Tetraodon nigroviridis* Elovl4 in the other (82.4 % identity). Identity scores within these two groups are higher than that of zebrafish Elovl4 proteins when compared to each other (73.8 % identity). Differentiation among fish Elovl4 proteins is reflected in the phylogenetic analysis (Fig. 2), with zebrafish Elovl4a clustering together with *T. rubripes* Elovl4, and zebrafish Elovl4b more closely with pufferfish *T. nigroviridis* predicted Elovl4. All fish Elovl4 elongases group with the mammalian and bird orthologues, and separately from other members of the Elovl family such as Elovl2 and Elovl5 from fish and mammalian (Fig. 2).

Functional characterisation

The zebrafish putative Elovl4 elongases were functionally characterised by determining the FA profiles of *S. cerevisiae* transformed with pYES2 containing *elovl4* inserts isolated from ovary (*elovl4a*) and eye (*elovl4b*) and grown in the presence of potential FA substrates. To test the ability of zebrafish Elovl4 to elongate saturated VLC-FA, yeast transformed with pYES2 containing the putative *elovl4* coding region cDNAs or no insert (control) were incubated with lignoceric acid (24:0) (Table 2; Fig. 3). The results confirm that zebrafish Elovl4s are both involved in the biosynthesis of saturated VLC-FAs. Thus, control yeast transformed with empty vector and incubated with 24:0 (lignoceric acid) contained measurable amounts of 24:0 (9.2% of total saturates ≥ C24), 26:0 (80.2%) and 28:0 (7.5%), with traces of longer FAs up to C34 (Table 2). Importantly, *elovl4* transformed yeast showed a different profile of saturated FAs ≥ C24 compared to control yeast, with decreased contents of 26:0 and increased levels of 28:0 (3.5- and 4.5-fold, for *elovl4a* and *elovl4b*, respectively), 30:0 (13.7- and 10.1-fold, for *elovl4a* and *elovl4b*, respectively) and 32:0 (13.5- and 3.5-fold, for *elovl4a* and *elovl4b*, respectively) (Table 2). These results suggest that 26:0 is a preferred substrate for both zebrafish Elovl4 proteins.

In order to test the role of *D. rerio* Elovl4 elongases in VLC-PUFA biosynthetic pathway, yeast transformed with zebrafish Elovl4s were incubated with C20 (20:5n-3 and 20:4n-6) and C22 (22:5n-3, 22:4n-6 and 22:6n-3) PUFAs. The FA composition of the yeast transformed with pYES2 vector containing no insert is characterised by having only 16:0, 16:1n-7, 18:0 and 18:1n-9, together with whichever exogenous FA was added, consistent with *S. cerevisiae* possessing no PUFA elongase activity [34]. GC-MS analyses revealed that zebrafish Elovl4a elongated 20:5n-3 and 20:4n-6 with up to 16.0 % and 20.3 % of each converted, respectively (Table 3). Elovl4a elongated

C22 PUFA substrates to a much lower extent (Table 3). Zebrafish Elovl4b, however, showed higher activity than Elovl4a towards 20:5n-3 and 20:4n-6, but especially towards C22 substrates 22:5n-3 and 22:4n-6. Conversions produced by *elovl4b*-transformed yeast included polyenes up to C36, with C32 PUFA consistently being the most abundant product (Table 3; Fig. 4). It is noteworthy that both zebrafish Elovl4 elongases are able to convert 20:5n-3 or 22:5n-3 to 24:5n-3, an intermediate substrate for Δ6 fatty acyl desaturase involved in 22:6n-3 (DHA) synthesis. However, in contrast zebrafish Elovl4s have virtually no activity towards DHA itself (Fig. 4C).

Spatial-temporal expression of zebrafish elovl4 genes

Temporal expression of *elovl4a* and *elovl4b* were studied by RT-PCR on cDNA samples obtained from embryos at different developmental stages from 0 to 7 dpf (Fig. 5). Results reveal that the two genes are expressed from the zygote stage, with transcripts detected throughout embryonic development (Fig. 5).

To determine the spatial expression patterns of *elovl4a* and *elovl4b*, an *in situ* whole-mount hybridisation time course was performed using wild-type zebrafish embryos. *Elovl4a* was widely distributed in the head region of 24 (Fig. 6A), 48 and 72 hpf embryos (data not shown). Unlike *elovl4a*, *elovl4b* was specifically expressed in the pineal gland (epiphysis) and the photoreceptor cell layer of the retina (Fig 7A-H). *Elovl4b* transcripts first appear in the pineal gland at 24 hpf (Fig. 7A, B), and remain in this site until around 48 hpf (Fig. 7C, D). At 48 hpf, *elovl4b* hybridisation signal also appears in the ventral area of developing retina (Fig. 7C, E). At 72 hpf, *elovl4b* transcripts become localised in the ventral portion of the retina photoreceptor cell layer, in the so-called ‘‘ventral patch’’(Fig. 7F, G, H). No signal was detected for sense control probes of *elovl4a* (Fig. 7B) and *elovl4b* genes (data not shown).

Tissue distribution of *elovl4* mRNAs in adult zebrafish was analysed by RT-PCR. *Elovl4a* transcripts were detected in most tissues analysed including liver, with muscle and adipose tissue not showing expression signal (Fig. 8). A more restricted pattern was observed for *elovl4b*, with high expression found in eye, ovary and testis (Fig. 8).

Discussion

The overall objective is to elucidate the molecular mechanisms controlling long-chain polyunsaturated fatty acid (LC-PUFA) biosynthesis in developing vertebrates as these fatty acids have critical biological functions during early ontogeny [39-42]. In a recent study investigating the activation of genes involved in the LC-PUFA biosynthesis pathway during zebrafish embryogenesis [43], we functionally characterised an Elovl2-like elongase that efficiently elongated C20 and C22 PUFA, and so had different substrate specificity to the formerly cloned Elovl5-like elongase [34], which was more active on C18 and C20 PUFA. In the present study, we characterised zebrafish Elovl4a and Elovl4b elongases, two further members of the Elovl protein family involved in fatty acid elongation in this vertebrate model.

Human ELOVL4, thus far being the only Elovl4-like protein functionally characterised, was demonstrated to participate in the biosynthesis of saturated VLC-FA ≥ C28 [17]. Decreased proportions of 26:0 and concomitant increased percentages of 28:0 and 30:0 in zebrafish *elovl4*-transformed yeast suggests that both zebrafish Elovl4s are involved in the synthesis of 28:0 and 30:0 from 26:0. Thus, Elovl4a and Elovl4b appear capable of producing saturated VLC-FA up to C36 from shorter-chain fatty acids. This is consistent with the conversions shown by human ELOVL4. Cell lines not naturally expressing *ELOVL4* showed decreased 26:0 levels and increased

levels of 28:0 and 30:0 when transformed with human *ELOVL4* [17]. Similar conclusions were obtained in genetically engineered mice lacking a functional Elovl4 protein, which showed increased levels of C26 FA and depletion of ≥C28 in lipids of the epidermal stratum corneum that altered the skin barrier function, and ultimately caused dehydration and perinatal death [12-15]. Apart from the essential role of Elovl4 for the formation of saturated ≥C28, ELOVL4 is also required for biosynthesis of VLC-PUFA [17,44], and so represents the first Elovl protein with dual substrate specificity for saturated and unsaturated VLC-FA [45].

The role of both zebrafish Elovl4 proteins in VLC-PUFA biosynthesis shows particular differences compared not only to mammalian Elovl4 proteins, but also to each other. On one hand, zebrafish Elovl4a does not appear to take part in the VLC-PUFA biosynthetic pathway, as only relevant conversions were observed on C20 PUFA substrates, with C22 PUFA remaining virtually unmodified. In contrast, zebrafish Elovl4b is very active towards both C20 and C22 PUFA substrates, producing polyenes up to C36 of the n-3 and n-6 series. This is in agreement with previous studies on human ELOVL4, which was seen to produce VLC-PUFAs [17], and mutated *Elovl4*-knockin mice showing deficiencies in C32-C36 phosphatidylcholines in retina [16]. However, contrary to human ELOVL4, zebrafish Elovl4b may participate in the biosynthesis of DHA, as it is able to convert 22:5n-3 to 24:5n-3, which can be further desaturated and chain-shortened to form DHA [46]. This role of Elovl4 in fish might be crucial in marine species, where lack of Elovl2 has been speculated to be one possible cause of their low LC-PUFA biosynthetic capability [43,47].

Functional characterisation of enzymes involved in the LC-PUFA biosynthetic pathway in zebrafish including C≥24 allows us to predict all the conversions

occurring from dietary essential C18 PUFA, 18:3n-3 and 18:2n-6 (Fig. 9). Together with desaturation and elongation steps performed by the dual Δ6/Δ5 fatty acyl desaturase (Δ6/Δ*5*Fad) [33], and the two elongases Elovl5 [34] and Elovl2 [43], the newly characterised Elovl4 proteins augment the scheme, with Elovl4a able to elongate C20 PUFAs, whilst Elovl4b can elongate C22 and even longer PUFA, appearing as the primary elongase for the production of VLC-PUFA in zebrafish. Although mouse ELOVL2 has been shown to participate in the synthesis of n-6 VLC-PUFA in testis [48], the zebrafish orthologue only produces products up to C26, with minor rates beyond that [43]. It is interesting to note that *D. rerio* Elovl4b has activity towards 20:5n-3 and 22:5n-3 but not DHA, the latter being only marginally elongated. This is consistent with previous investigations in mammalian retina where radiolabeled 20:5n-3 or 22:5n-3 were actively elongated, whereas DHA remained essentially unmodified and was directly esterified into phospholipids without further metabolism [49,50]. Although not directly tested in the present study, similar conversion patterns are expected to occur for the n-6 series, with 20:4n-6 and 22:4n-6 but not 22:5n-6 being elongated to VLC-PUFA (Fig. 9).

Differences in the AA sequences of the Elovl4a and Elovl4b proteins might be the basis of the distinct functional roles discussed above. Phylogenetic analyses revealed that teleost Elovl4 proteins, besides clustering separately from other vertebrate Elovl4s, form two separate groups themselves, with zebrafish Elovl4a and *Takifugu rubripes* Elovl4 separated from zebrafish Elovl4b and *Tetraodon nigroviridis* Elovl4. Indeed, identity scores within each group (81.1% and 82.4 %, respectively) are higher than that between zebrafish Elovl4a and Elovl4b (73.8 % identity). These results, together with the different substrate specificities and embryonic expression patterns shown by zebrafish Elovl4s, suggest that, whereas Elovl4b is a common Elovl4-like

protein similar to mammalian orthologues, zebrafish Elovl4a may represent a distinct member of the Elovl protein family in *D. rerio*, that may possibly extend to other teleosts. Cloning and functionally characterisation of further Elovl4 elongases from fish are required to confirm this possibility.

Elovl4 has been considered a crucial gene in early development of vertebrates. In addition to its role in the synthesis of important components for normal skin permeability barrier in mammals, essentiality of *Elovl4* in early developmental stages has been indicated by the fact that it is expressed prior to organogenesis in mouse embryos [51]. Similarly, our data confirm that both *elovl4a* and *elovl4b* are expressed before early organogenesis in zebrafish, which occurs from segmentation period (10 hpf) [32]. Moreover, zebrafish *elovl4a* and *elovl4b* transcripts are evident throughout embryogenesis of zebrafish, including stages before midblastula transition (512 cell stage, 2.75 hpf) when embryonic gene activation occurs [32]. Therefore, maternal transfer of mRNA occurs for both *elovl4* genes, as previously reported for genes involved in the biosynthesis of LC-PUFA from dietary essential 18:3n-3 and 18:2n-6 [43]. The maternal role can thus expand beyond the deposition of preformed C20-22 LC-PUFA and, possibly, VLC-PUFA in the yolk, by transferring mRNA transcripts that can potentially be translated to active proteins.

Preliminary data from zebrafish transcriptome *in situ* hybridisation screening had suggested that the putative *elovl4* genes showed different spatial-temporal expression patterns during embryonic development [52]. This is now confirmed by our WISH analyses. Zebrafish *elovl4a* is expressed in neuronal tissues from 24 hpf onwards, with possibly CNS and cranial ganglia being active metabolic tissues [53]. A similar expression pattern was previously shown for *elovl5* and the dual Δ6/Δ*5fad* [43], both genes encoding enzymes involved in LC-PUFA biosynthesis [54]. In adulthood

elovl4a expression spreads to most tissues including liver, the latter not being generally regarded as a major metabolic site for the synthesis of VLC-FA [17,44,51]. This further suggests that zebrafish Elovl4a differs from mammalian orthologues, whose expression is essentially restricted to retina, brain, skin and testis [17,51].

During embryonic development zebrafish *elovl4b* mRNA localises specifically in retina and epiphysis (pineal gland). These findings are in agreement with transcriptome analyses of zebrafish retina [55] and pineal gland [56] demonstrating the presence of *elovl4b* mRNA in early developmental stages. Teleostei retina and epiphysis have been hypothesised to have a common evolutionary origin [57], with both tissues possessing photoreceptor cells where expression of *elovl4* genes are likely to occur [51,55,58]. Thus we present compelling evidence that, similar to mammals, zebrafish photoreceptor cells actively express *elovl4b* from embryonic stages. Although expression in pinealocyte photoreceptors could not be characterised, the results suggest a prominent metabolic role of epiphysis from early developmental stages, thus expanding the capacity of C20-22 PUFA metabolism in adult fish [59,60]. Expression of *elovl4b* remains in adult fish epiphysis [56], and also extends to other tissues with ovaries and testes showing strong expression signals.

Overall our results demonstrate that the two Elovl4 proteins found in zebrafish show marked differences in specificity and expression. Whereas Elovl4b resembles other mammalian orthologues in terms of function and expression patterns, Elovl4a may represent an alternative elongase not yet described in vertebrates and whose physiological roles require further investigation.

Acknowledgements

This research and OM were supported by a Marie Curie Intra European Fellowship within the 7th European Community Framework Programme (PIEF-GA-2008-220929, COBIAGENE). JR, JMCR and AF were funded by projects from the Spanish Ministry of Science and Innovation (AGL2008-00392/ACU, AGL2007-65744-C03-02 and Consolider-Ingenio-CSD2007-00002).

References

[1]D.H. Nugteren, The enzymatic chain elongation of fatty acids by rat-liver microsomes. Biochim. Biophys. Acta 106 (1965) 280-290.

[2]A. Jakobsson, R. Westerberg, A. Jacobsson, Fatty acid elongases in mammals: Their regulation and roles in metabolism, Prog. Lipid Res. 45 (2006) 237-249.

[3]K. Tamura, A. Makino, F. Hullin-Matsuda, T. Kobayashi, M. Furihata, S. Chung, S. Ashida, T. Miki, T. Fujioka, T. Shuin, Y. Nakamura, H. Nakagawa, Novel lipogenic enzyme ELOVL7 is involved in prostate cancer growth through saturated long-chain fatty acid metabolism, Cancer. Res. 69 (2009) 8133-8140.

[4]A.E. Leonard, S.L. Pereira, H. Sprecher, Y.S. Huang Elongation of long-chain fatty acids, Prog. Lipid Res. 43 (2004) 36-54.

[5]K. Zhang, M. Kniazeva, M. Han, W. Li, Z. Yu, Z. Yang, Y. Li , M.L. Metzker, R. Allikmets, D.J. Zack, L.E. Kakuk, P.S. Lagali, P.W. Wong, I.M. MacDonald, P.A. Sieving, D.J. Figueroa, C.P. Austin, R.J. Gould, R. Ayyagari, K. Petrukhin, A 5-bp deletion in ELOVL4 is associated with two related forms of autosomal dominant macular dystrophy, Nat. Genet. 27 (2001) 89 – 93.

[6]P.S. Bernstein, J. Tammur, N. Singh, A. Hutchinson, M.Dixon, C.M.Pappas, N.A. Zabriskie, K. Zhang, K. Petrukhin, M. Leppert, R. Allikmets, Diverse macular dystrophy phenotype caused by a novel complex mutation in the ELOVL4 gene. Invest. Ophthalmol. Vis. Sci. 42 (2001) 3331–3336.

[7]A. Maugeri, F. Meire, C.B. Hoyng, C. Vink, N. Van Regemorter, G. Karan, Z. Yang, F.P. Cremers, K. Zhang, A novel mutation in the ELOVL4 gene causes autosomal dominant Stargardt-like macular dystrophy. Invest. Ophthalmol. Vis. Sci. 45 (2004) 4263 - 4267.

[8]C. Grayson, R.S. Molday, Dominant negative mechanism underlies autosomal dominant Stargardt-like macular dystrophy linked to mutations in ELOVL4. J. Biol. Chem. 280 (2005) 32521–32530.

[9]G. Karan G, et al. Lipofuscin accumulation, abnormal electrophysiology, and photoreceptor degeneration in mutant ELOVL4 transgenic mice: A model for macular degeneration. Proc. Natl. Acad. Sci. USA 102 (2005) 4164 – 4169.

[10]V. Vasireddy, C. Vijayasarathy, J. Huang, X.F.,Wang, M.M. Jablonski, H.R. Petty, P.A. Sieving, R. Ayyagari, Stargardt-like macular dystrophy protein ELOVL4 exerts a dominant negative effect by recruiting wild-type protein into aggresomes. Mol. Vis. 11 (2005) 665 – 676.

[11]H.W. Cook, R.C.R. McMaster, Fatty acid desaturation and chain elongation in eukaryotes. In: Vance D.E. and Vance J.E. (Eds.), Biochemistry of Lipids, Lipoproteins and Membranes, Elsevier, Amsterdam, 2004.

[12]D.J. Cameron, Z. Tong, Z. Yang, J. Kaminoh, S. Kamiyah, H. Chen, J. Zeng, Y. Chen, L. Lou, K. Zhang, Essential role of Elovl4 in very long chain fatty acid synthesis, skin permeability barrier function, and neonatal survival, Int. J. Biol. Sci. 3 (2007) 111-119.

[13]W. Li, Y. Chen, D.J. Cameron, C. Wang, G. Karan, Z. Yang, Y, Zhao, E. Pearson, H. Chen, C. Deng, K. Howes, K. Zhang, *Elovl4* haploinsufficiency does not induce early onset retinal degeneration in mice, Vision Res. 47 (2007) 714-722.

[14]W. Li, R. Sandhoff, M. Kono, P. Zerfas, V. Hoffman, B.C-H. Ding, R.L. Proia, C-X. Deng, Depletion of ceramides with very long chain fatty acids causes defective skin permeability barrier function, and neonatal lethality in ELOVL4 deficient mice, Int. J. Biol. Sci. 3 (2007) 120-128.

[15]V. Vasireddy, Y. Uchida, N. Salem Jr, S.Y. Kim, M.N.A. Mandal, G. Bhanuprakash Reddy, R. Bodepudi, N.L. Alderson, J.C. Brown, H. Hama, A. Dlugosz, P.M. Elias, W.M. Holleran, R. Ayyagari, Loss of functional ELOVL4 depletes very long-chain fatty acids (≥C28) and the unique ω-O-acylceramides in skin leading to neonatal death, Hum. Mol. Genet. 16 (2007), 471-482.

[16]A. McMahon, S.N. Jackson, A.S. Woods, W. Kedzierski, A Stargardt disease-3 mutation in the mouse Elovl4 gene causes retinal deficiency of C32-C36 acyl phosphatidylcholines, FEBS Lett. 581 (2007) 5459-5463.

[17]M.–P. Agbaga, R.S. Brush, M.N.A. Mandal, K. Henry, M.H. Elliott, R.E. Anderson, Role of Stargardt-3 macular dystrophy protein (ELOVL4) in the biosynthesis of very long chain fatty acids, Proc. Natl. Acad. Sci. USA, 105 (2008) 12843-12848.

[18]Y. Uchida, W.M. Holleran, Omega-O-acylceramide, a lipid essential for mammalian survival, J. Dermatol. Sci. 51 (2008) 77-87.

[19]M.I. Aveldaño, A novel group of very long chain polyenoic fatty acids in dipolyunsaturated phosphatidylcholines from vertebrate retina. J. Biol. Chem. 262 (1987) 1172–1179.

[20]M.I. Aveldaño, Phospholipid species containing long and very long polyenoic fatty acids remain with rhodopsin after hexane extraction of photoreceptor membranes. Biochemistry 27 (1988) 1229-1239.

[21]B.S. Robinson, D.W. Johnson, A. Poulos, Unique molecular species of

phosphatidylcholine containing very-long-chain (C24-C38) polyenoic fatty acids in rat brain. Biochem. J. 265 (1990) 763-7.

[22]A. Poulos, Very long chain fatty acids in higher animals – A review, Lipids 30 (1995) 1-14.

[23]N.E. Furland, E.N. Maldonado, M.I. Aveldaño, Very long chain PUFA in murine testicular triglycerides and cholesterol esters, Lipids 38 (2003) 73-80.

[24]N.E. Furland, G.M. Oresti, S.S. Antollini, A. Venturino, E.N. Maldonado, M.I. Aveldaño, Very long-chain polyunsaturated fatty acids are the major acyl groups of sphingomyelins and ceramides in the head of mammalian spermatozoa, J. Biol. Chem. 282 (2007) 18151-18161.

[25]N.E. Furland, E.N. Maldonado, P. Ayuza-Aresti, M.I. Aveldaño, Changes in lipids containing long- and very long-chain polyunsaturated fatty acids in cryptorchid rat testes, Biol. Reprod. 77 (2007) 181-188.

[26]A. McMahon, W. Kedzierski, Polyunsaturated extremely long chain C28-C36 fatty acids and retinal physiology, Br. J. Ophthalmol. (in press) doi: 10.1136/bjo.2008.149286

[27]S.A. Farber, M. Pack, S.-Y. Ho, I.D. Johnson, D.S. Wagner, R. Dosch, M.C. Mullins, H.S. Hendrickson, E.K. Hendrickson, M.E. Halpern, Genetic analysis of digestive physiology using fluorescent phospholipid reporters, Science 292 (2001) 1385–1388.

[28]S.-Y. Ho, J.L. Thorpe, Y. Deng, E. Santana, R.A. DeRose, S.A. Farber, Lipid metabolism in zebrafish, Methods Cell Biol. 76 (2004) 87-108.

[29]A. Schlegel, D.Y.R. Stainer, Microsomal triglyceride transfer protein is required for yolk lipid utilization and absorption of dietary lipids in zebrafish larvae, Biochemistry 45 (2006) 15179-15187.

[30]Y. Song, R.D. Cone, Creation of a genetic model of obesity in a teleost, FASEB J. 21 (2007) 2042–2049.

[31]M. Westerfield, The Zebrafish Book: A guide for the laboratory use of Zebrafish (*Danio rerio*), 5th ed, Univ. of Oregon Press, Eugene, 2007.

[32]C.B. Kimmel, W.W. Ballard, S.R. Kimmel, B. Ullmann, T.F. Schilling, Stages of embryonic development of the zebrafish, Dev. Dyn. 203 (1995) 253-310.

[33]N. Hastings, M. Agaba, D.R. Tocher, M.J. Leaver, J.R. Dick, J.R. Sargent, A.J. Teale, A Vertebrate Fatty Acid Desaturase with Δ5 and Δ6 Activities, Proc. Natl. Acad. Sci. USA 98 (2001) 14304-14309.

[34]M. Agaba, D.R. Tocher, C. Dickson, J.R. Dick, A.J. Teale, Zebrafish cDNA encoding multifunctional fatty acid elongase involved in production of eicosapentaenoic (20:5n-3) and docosahexaenoic (22:6n-3) acids, Mar. Biotechnol. 6 (2004) 251-261.

[35]I. Singh, Y. Kishimoto, Effect of cyclodextrins on the solubilization of lignoceric acid, ceramide, and cerebroside, and on the enzymatic reactions involving these compounds, J. Lipid Res. 24 (1983) 662-665.

[36]N. Saitou, M. Nei, The neighbor-joining method. A new method for reconstructing phylogenetic trees, Mol. Biol. Evol. 4 (1987) 406-425.

[37]R. Tang, A. Dodd, D. Lai, W.C. McNabb, D.R. Love, Validation of zebrafish (*Danio rerio*) reference genes for quantitative real-time RT-PCR normalization, Acta Biochim. Biophys. Sin. 39 (2007) 384-390.

[38]J. Rotllant, D. Liu. Y-L. Yan, J.H. Postlethwait, M. Westerfield, S-J. Du, Sparc functions in morphogenesis of pharyngeal skeleton and inner ear, Matrix Biol. 27 (2008) 561-572.

[39]M.T. Clandinin, Brain development and assessing the supply of polyunsaturated

fatty acid, Lipids 34 (1999) 131-137.

[40]S.M. Innis, H. Sprecher, D. Hachey, J. Edmond, R.E. Anderson, Neonatal polyunsaturated fatty acid metabolism, Lipids 34 (1999) 139-149.

[41]L. Lauritzen, H.S. Hansen, M.H. Jørgensen, K.F. Michaelsen, The essentiality of long chain n-3 fatty acids in relation to development and function of the brain and retina, Prog. Lipid Res. 40 (2001) 1-94.

[42]J.L. Watts, E. Phillips, K.R. Griffing, J. Browse, Deficiencies of C20 polyunsaturated fatty acids cause behavioral and developmental defects in *Caenorhabditis elegans* fat-3 mutants, Genetics 163 (2003) 581-589.

[43]Ó. Monroig, J. Rotllant, E. Sánchez, J.M. Cerdá-Reverter, D.R. Tocher, Expression of long-chain polyunsaturated fatty acid (LC-PUFA) biosynthesis genes during zebrafish *Danio rerio* early embryogenesis, Biochim. Biophys. Acta 1791 (2009) 1093–1101.

[44] M. Tikhonenko, T.A. Lydic, Y. Wang, W. Chen, M. Opreanu, A. Sochacki, K.M. McSorley, R.L. Renis, T. Kern, D.B. Jump, G.E. Reid, J.V. Busik, Remodeling of Retinal Fatty Acids in an Animal Model of Diabetes: A Decrease in Long-Chain Polyunsaturated Fatty Acids Is Associated With a Decrease in Fatty Acid Elongases Elovl2 and Elovl4, Diabetes 59 (2010) 219-227.

[45]H. Guillou, D. Zadravec, P. G.P. Martin, A. Jacobsson. The key roles of elongases and desaturases in mammalian fatty acid metabolism: Insights from transgenic mice. Prog. Lipid Res. 49 (2010) 186-199.

[46]S. Ferdinandusse, S. Denis, C.W.T. van Roermund, R.J.A. Wanders, G. Dacremont, Identification of the peroxisomal-oxidation enzymes involved in the degradation of long-chain dicarboxylic acids, J. Lipid Res. 45 (2004) 1104-1111.

[47]S. Morais, Ó. Monroig, X. Zheng, M.J. Leaver, D.R. Tocher, Highly unsaturated

fatty acid synthesis in Atlantic salmon: characterization of Elovl5- and Elovl2-like elongases, Mar. Biothecnol. 11 (2009) 627–639.

[48]D. Zadravec, Metabolic significance of fatty acid elongation, PhD Thesis, Stockholm University, Stockholm, Sweden 2010.

[49]N.P. Rotstein, G.L. Pennacchiotti, H. Sprecher, M.I. Aveldaño, Active synthesis of $C_{24:5,n-3}$ fatty acid in retina, Biochem. J. 316 (1996) 859-864.

[50]M. Suh, M.T. Clandinin, 20:5n-3 but not 22:6n-3 is a preferred substrate for synthesis of n-3 very-long-chain fatty acids (C24–C36) in retina, Curr. Eye Res. 30 (2005) 959–968.

[51]M.N.A. Mandal, R. Ambasudhan, P.W. Wong, P.J. Gage, P.A. Sieving, R. Ayyagari, Characterization of mouse orthologue of *ELOVL4*: genomic organization and spatial and temporal expression, Genomics 83 (2004) 626-635.

[52]B. Thisse, V. Heyer, A. Lux, V. Alunni, A. Degrave, I. Seiliez, J. Kirchner, J.P. Parkhill, C. Thisse, Spatial and temporal expression of the zebrafish genome by large scale in situ hybridization screening, Methods Cell Biol. 77 (2004) 505–519.

[53]B. Thisse, C. Thisse, Fast Release Clones: A High Throughput Expression Analysis. ZFIN Direct Data Submission (2004) (http://zfin.org).

[54]H. Sprecher, Metabolism of highly unsaturated n-3 and n-6 fatty acids, Biochim Biophys. Acta 1486 (2000) 219-231.

[55]Y.F. Leung, J.E. Dowling, Gene Expression Profiling of Zebrafish Embryonic Retina, Zebrafish 2 (2005) 270-283.

[56]R. Toyama, X. Chen, N. Jhawar, E. Aamar, J. Epstein, N. Reany, S. Alon, Y. Gothilf, D.C. Klein, I.B. Dawid, Transcriptome analysis of the zebrafish pineal gland, Dev. Dyn. 238 (2009) 1813–1826.

[57]J. Falcon, Cellular circadian clocks in the pineal. Prog Neurobiol 58 (1999) 121–

162.

[58]X-M. Zhang, Z. Yang, G. Karan, T. Hashimoto, W. Baehr, X-J. Yang, K. Zhang, *Elovl4* mRNA distribution in the developing mouse retina and phylogenetic conservation of *Elovl4* genes, Mol. Vis. 9 (2003) 301-307.

[59]J. Falcón, R.J. Henderson, Incorporation, distribution, and metabolism of polyunsaturated fatty acids in the pineal gland of rainbow trout (*Oncorhynchus mykiss*) in vitro, J. Pineal Res. 31 (2001) 127-137.

[60]A. Catalá, The function of very long chain polyunsaturated fatty acids in the pineal gland, Biochim Biophys. Acta 1801 (2010) 95-99.

Figures

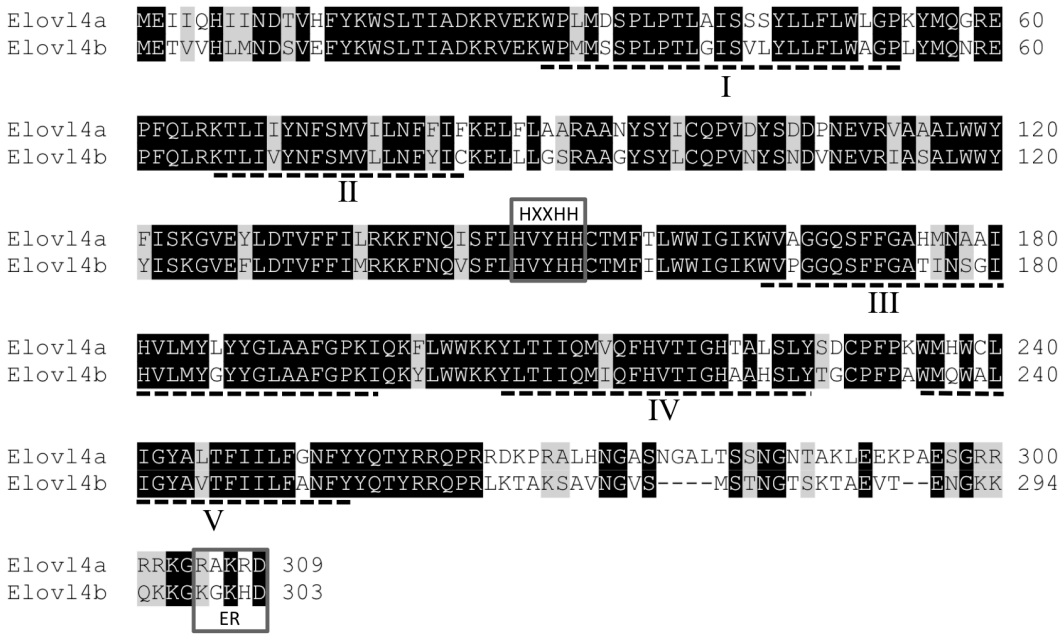

Fig. 1. ClustalW2 alignment of the deduced amino acid sequences of zebrafish Elovl4a and Elovl4b. Identical residues are shaded black and similar residues (based on the Gonnet matrix, using ClustalW2 default parameters) are shaded grey. Indicated are the conserved histidine box motif HXXHH, five (I-V) putative membrane-spanning domains, and the putative endoplasmic reticulum (ER) retrieval signal [58].

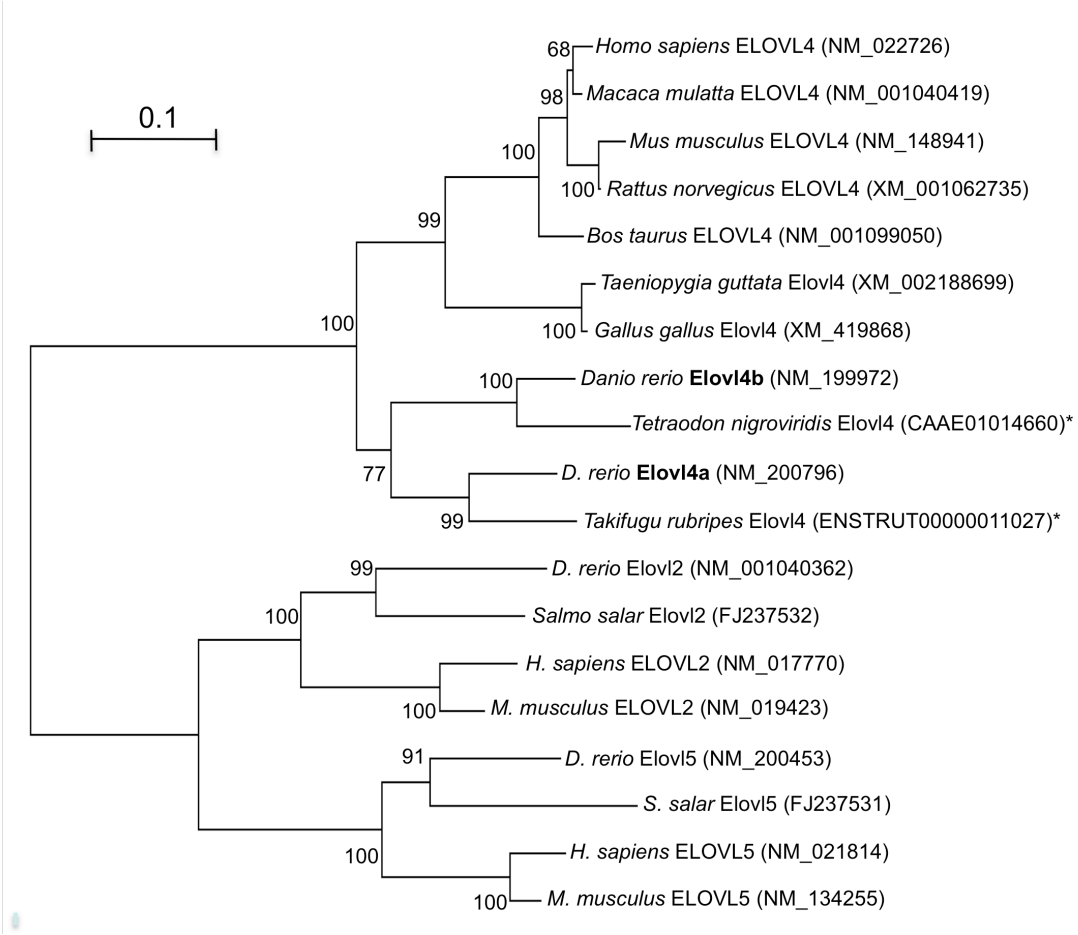

Fig. 2. Phylogenetic tree comparing zebrafish Elovl4 proteins, with other Elovl4 orthologues, Elovl2- and Elovl5-like elongases. The tree was constructed using the Neighbour Joining method [36] with MEGA4. The horizontal branch length is proportional to amino acid substitution rate per site. The numbers represent the frequencies (%) with which the tree topology presented was replicated after 1000 iterations.

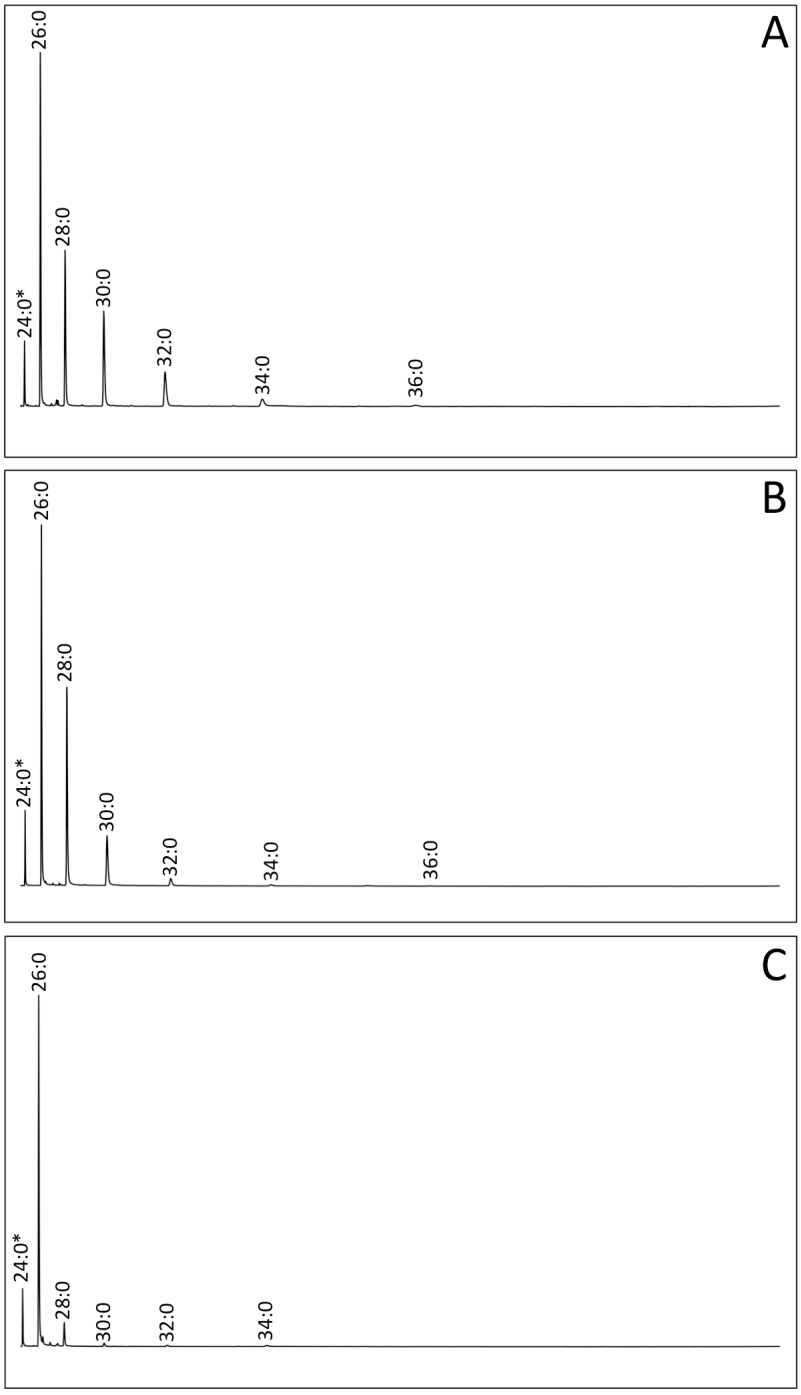

Fig. 3. Role of zebrafish Elovl4 elongases in the biosynthesis of saturated very long-chain fatty acids (VLC-FA). Yeast (*Saccharomyces cerevisiae*) transformed with pYES2 vector containing the ORF of *elovl4a* (A) and *elovl4b* (B) as inserts were grown in the presence of lignoceric acid 24:0, and fatty acid composition determined. Substrate 24:0 ("*") and its corresponding elongated products are indicated

accordingly. Saturated VLC-FA from control yeast transformed with empty pYES2 are shown in panel C. Vertical axis, FID response; horizontal axis, retention time.

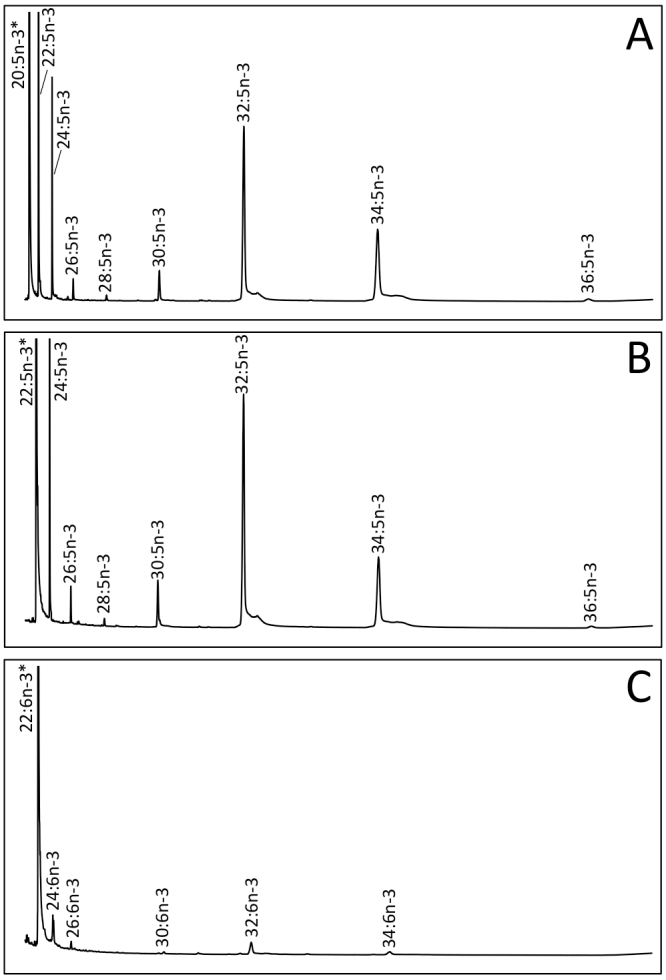

Fig. 4. Role of zebrafish Elovl4b elongase in the biosynthesis of very long-chain fatty acids (VLC-PUFA). Yeast (*S. cerevisiae*) transformed with pYES2 vector containing the ORF of *elovl4b* as insert were grown in the presence of PUFA substrates 20:5n-3 (A), 22:5n-3 (B) and 22:6n-3 (C), and fatty acid composition determined. Substrates ("*") and their corresponding elongated products are indicated accordingly in panels A-F. Vertical axis, FID response; horizontal axis, retention time.

Fig. 5. RT-PCR analyses of the temporal expression patterns of *elovl4a* and *elovl4b* during zebrafish early embryogenesis (0 hours to 7 days post-fertilisation at 28.5 ºC).

Expression of the housekeeping gene *β-actin* is also shown. h, hours post-fertilisation; d, days post-fertilisation; NTC, no template control.

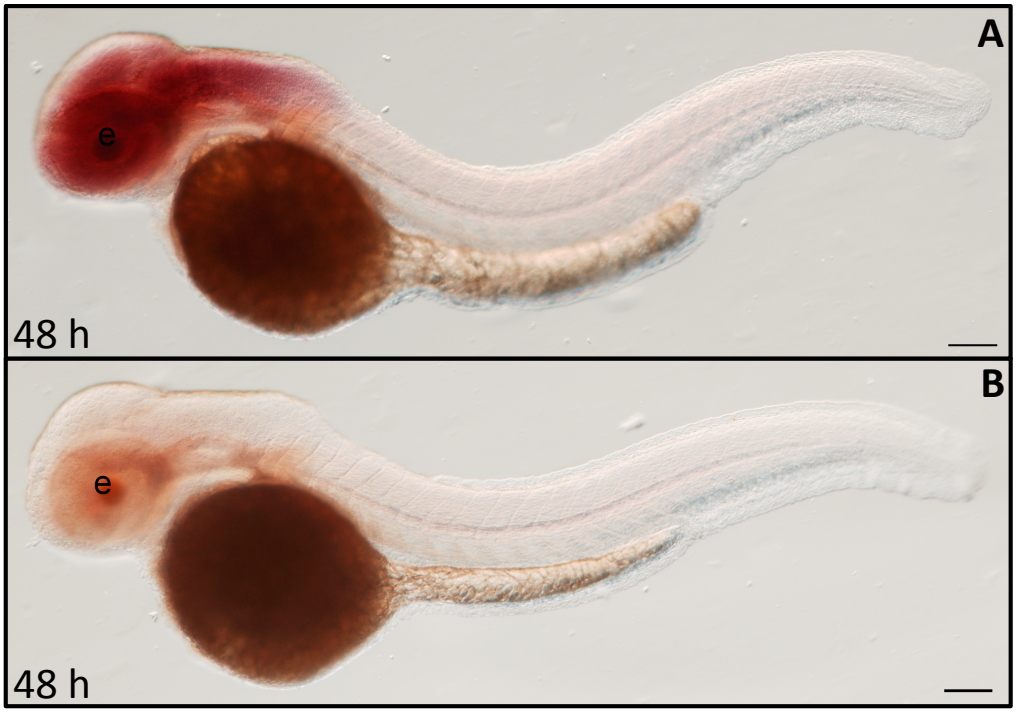

Fig. 6. Whole-mount *in situ* hybridisation showing the expression patterns of *elovl4a* in 48 hpf embryos. Embryos were hybridised with either antisense (A) or sense probes (B). Strong signal was observed in the head region of 48 hpf embryos when antisense probe was used (A), but no signal was observed for sense probe (B). Lateral views, dorsal upward, anterior to the left. Abbreviations: e: eye. Scale bars: 100 μm.

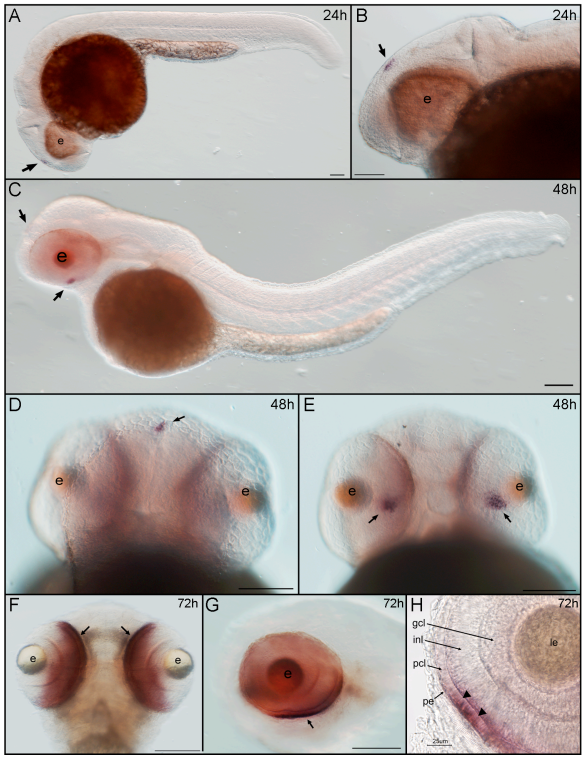

Fig. 7. Spatial-temporal expression pattern of *elovl4b* by whole-mount *in situ* hybridisation. A, B: *Elovl4b* transcripts appear at 24 hpf in the pineal gland and remain in this site until around 48 hpf (black arrows). Lateral view, anterior left up. C-E: Lateral view, anterior left up of 48 hpf embryos shown in (C). Arrows point to the pineal gland and ventral area of the retina expression. (D) Dorsal view, anterior up of 48 hpf embryo of *elovl4b* staining the pineal gland (black arrows). (E) ventral view, anterior up of 48 hpf embryo of *elovl4b* staining in the ventral area of developing retina (black arrows). F, G: *Elovl4b* expression in the retinal epithelium (black arrows) is localised ventrally at the edges (72 hpf). Lateral view, anterior left up (F) and ventral view, anterior up (G). H: At 72 hpf, the strongest *elovl4b* expression is present in the ventral portion of the retina photoreceptor cell layer, in the so-called ‘‘ventral patch’’ (arrowheads). Lateral view, anterior up. No signal was detected for sense control probes (data not shown). Abbreviations: e, eye; le, lens; pcl, photoreceptor cell layer; inl, inner nuclear layer; gcl, ganglion cell layer; pe, pigment epithelium. Scale bars: 100 μm (A,B,C,D,E,F,G), 25 μm (H).

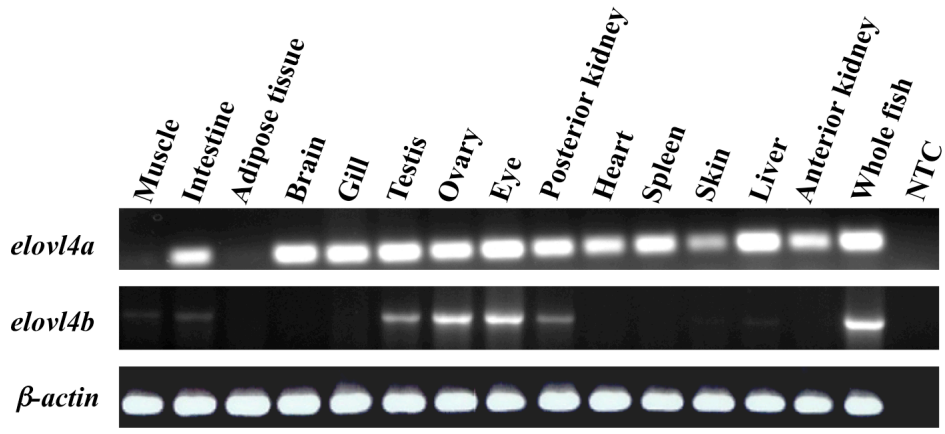

Fig. 8. RT-PCR analyses showing the tissue distribution of *elovl4a* and *elovl4b* transcripts in zebrafish adults. Expression of the housekeeping gene *β-actin* is also shown. NTC, no template control.

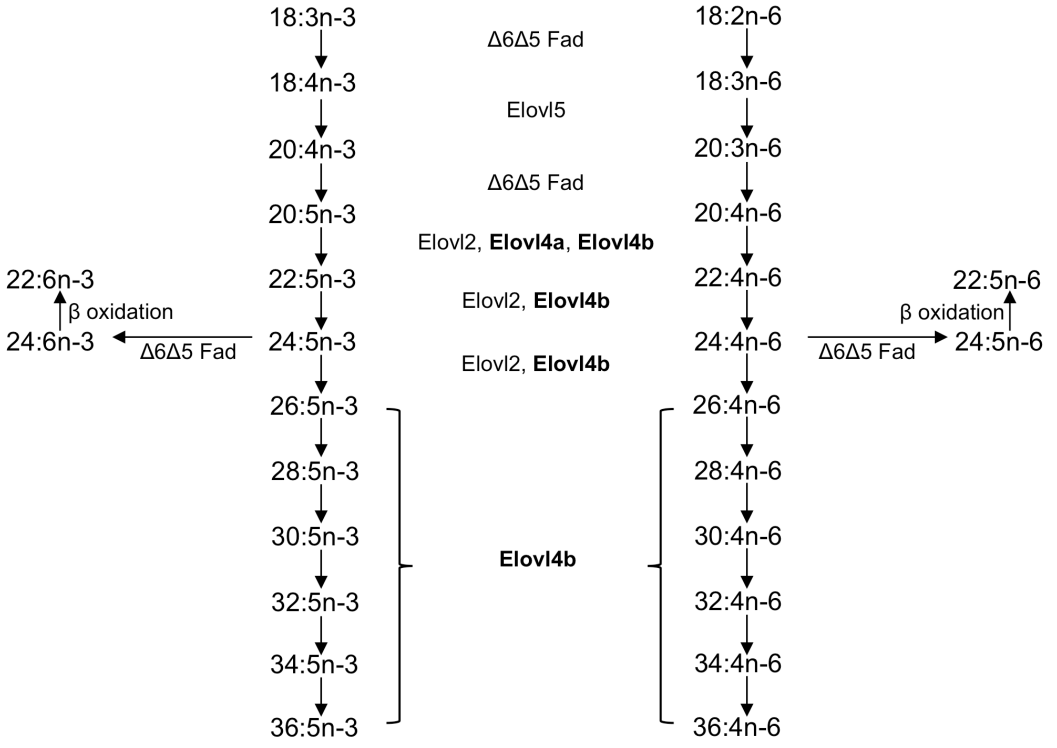

Fig. 9. The long-chain polyunsaturated fatty acid biosynthetic pathway from 18:3n-3 and 18:2n-6. Enzymatic activities shown in the scheme are predicted from heterologous expression in *S. cerevisiae* of the dual Δ6/Δ5 fatty acyl desaturase

(Δ6/Δ5Fad) [33], and Elovl5 [34] and Elovl2 [43] elongases. Steps catalysed by the newly characterised Elovl4a and Elovl4b are also shown.

Tables

Table 1. Sequence of the primer pairs used, size of the fragment produced and accession number of the sequence used as reference for primer design, for *elovl4* ORFs cloning and reverse transcriptase PCR (RT-PCR) performed in zebrafish embryos and adult tissues.

Aim	Transcript	Primer	Primer sequence	Fragment	Accession No[1].
ORF cloning	*elovl4a*	Elovl4aVF	5'-CCCAAGCTTAGGATGGAGATCATCCAGCACA-3'	951 bp	NM_200796
		Elovl4aVR	5'-CCGCTCGAGTTAATCGCGCTTCGCTCTGC-3'		
		Elovl4aU5F	5'-GACGACTGTGAGGATCTGAG-3'	1003 bp	
		Elovl4aU3E	5'-TTGTTCACGATGCTCTCGCT-3'		
	elovl4b	Elovl4bVF	5'-CCCAAGCTTAGGATGGAGACGGTCGTTCACC-3'	933 bp	NM_199972
		Elovl4bVR	5'-CCGCTCGAGTTAATCGTGCTTTCCTTTTCCTTT-3'		
		Elovl4bU5F	5'-CACGCGCTCGTAAGGATAAT-3'	2202 bp	
		Elovl4bU3E	5'-ACTGACGTTGCAAATCACGA-3'		
RT-PCR	*elovl4a*	Elovl4aF	5'-TGGATGCACTGGTGTCTGAT-3'	567 bp	NM_200796
		Elovl4aR	5'-CCTGGCCTGAGTTTTTGTGT-3'		
	elovl4b	Elovl4bF	5'-CACGCGCTCGTAAGGATAAT-3'	507 bp	NM_199972
		Elovl4bR	5'-GGATGAACATTGTGCAGTGG-3'		
	β-actin	β-ActinF	5'-CTCTTCCAGCCTTCCTTCCT-3'	246 bp	NM_131031
		β-ActinR	5'-CACCGATCCAGACGGAGTAT-3'		

[1] GenBank (http://www.ncbi.nlm.nih.gov/)

Table 2. Functional characterisation of zebrafish Elovl4 elongases: Role in biosynthesis of very long-chain saturated fatty acids (FA). Results are expressed as an area percentage of total saturated FA C≥24 found in yeast transformed with either zebrafish *elovl4* ORFs or empty pYES2 vector (Control).

FA	Elovl4a	Elovl4b	Control
24:0*	5.3	5.5	9.2
26:0	38.5	42.9	80.2
28:0	22.3	33.7	7.5
30:0	19.2	14.1	1.4
32:0	10.8	2.8	0.8
34:0	3.3	0.7	0.9
36:0	0.6	0.2	0.0

* Lignoceric acid used as exogenously added substrate.

Table 3. Functional characterisation of zebrafish Elovl4 elongases: conversions on polyunsaturated fatty acid (FA) substrates. Results are expressed as a percentage of total FA substrate converted to elongated product. Percentage of stepwise conversion into intermediary products of the elongation pathway is also shown.

FA substrate	Product	Elovl4a	Elovl4b	Activity
20:5n-3	22:5n-3	11.2	9.2	C20→22
	24:5n-3	2.8	3.3	C22→24
	26:5n-3	0.4	0.4	C24→26
	28:5n-3	0.0	0.1	C26→28
	30:5n-3	0.0	1.3	C28→30
	32:5n-3	0.2	11.6	C30→32
	34:5n-3	0.7	7.8	C32→34
	36:5n-3	0.5	0.4	C34→36
	Total	16.0	34.1	
20:4n-6	22:4n-6	11.5	9.0	C20→22
	24:4n-6	4.6	3.5	C22→24
	26:4n-6	1.0	0.8	C24→26
	28:4n-6	0.0	0.4	C26→28
	30:4n-6	0.2	4.7	C28→30
	32:4n-6	0.5	16.9	C30→32
	34:4n-6	2.6	2.8	C32→34
	36:4n-6	0.0	0.0	C34→36
	Total	20.3	38.1	
22:5n-3	24:5n-3	3.8	5.5	C22→24
	26:5n-3	0.4	0.6	C24→26
	28:5n-3	0.0	0.2	C26→28
	30:5n-3	0.0	1.7	C28→30
	32:5n-3	0.2	14.3	C30→32
	34:5n-3	0.5	7.2	C32→34
	36:5n-3	0.3	0.2	C34→36
	Total	5.2	29.8	
22:4n-6	24:4n-6	3.4	3.6	C22→24
	26:4n-6	0.7	0.4	C24→26
	28:4n-6	0.0	0.2	C26→28
	30:4n-6	0.1	2.8	C28→30
	32:4n-6	0.4	12.5	C30→32
	34:4n-6	2.2	3.6	C32→34
	36:4n-6	0.0	0.0	C34→36
	Total	6.8	23.1	
22:6n-3	24:6n-3	0.2	0.6	C22→24
	26:6n-3	0.0	0.0	C24→26
	28:6n-3	0.0	0.0	C26→28
	30:6n-3	0.0	0.1	C28→30
	32:6n-3	0.0	1.4	C30→32
	34:6n-3	0.0	0.5	C32→34
	36:6n-3	0.0	0.0	C34→36

Total	0.2	2.7